

Extraction of the Coronary Artery Tree in Cardiac Computer Tomographic Images Using Morphological Operators

M.A. Luengo-Oroz¹, M.J. Ledesma-Carbayo¹, J.J. Gómez-Diego²,
M.A. García-Fernández², M. Descó², and A. Santos¹

¹ Biomedical Image Technologies, ETSI Telecomunicación,
Universidad Politécnica de Madrid, 28040, Madrid, Spain

² Hospital General Universitario Gregorio Marañón,
C/Doctor Esquerdo 46, 28007, Madrid, Spain

Abstract. Quantitative measurements of the coronary artery tree substructures from Cardiac Multislice-CT data sets is an important goal to improve the diagnosis and treatment of coronary artery disease. This paper presents an algorithm based on morphological grayscale reconstruction through 2D slice images devoted to the extraction of the 3D coronary artery tree. The proposed procedure is conceived as a first step prior to the segmentation and inspection of interesting substructures in the coronaries. The correct extraction of the left coronary arteries has been validated in 9 CT-datasets with satisfactory results, particularly concerning speed and robustness.

1 Introduction

The conventional way of imaging coronary arteries is by using invasive coronary angiography, but this technique implies invasive clinical procedures and risks to the patient. Multislice CT (MSCT) imaging is a recent non-invasive imaging technique that provides high resolution data of the heart anatomy. An intravenous contrast agent is used to enhance the visibility of blood, and consequently the vessels. Areas containing the contrast agent are highlighted in the resultant output images as they have a larger Hounsfield value. Segmentation of the coronary arteries provide a valuable tool for clinicians interested in the detection and quantification of plaques, calcifications or stenosis. However, segmentation of the coronary tree is a difficult task due to low contrast conditions, the vicinity to the heart cavities, and its complex structure, including branching and curvatures. On the other hand, the clinical context demands minimal user interaction procedures, as well as fast and efficient algorithms.

In medical imaging, vessel segmentation (see a very complete review in [1]) is the core of many diagnosis systems that perform vessel analysis and visualization, and it may also be required in therapeutic tools such as computer-guided surgery. However, vessel segmentation is still an open problem and many methods have been proposed depending on the imaging modality, the human interaction required and many other factors. Concerning segmentation of the coronary

tree from MSCT, in [2] the segmentation is achieved using a combination of thresholding, region-growing, and morphological operations. Although a very good visualization interface is provided, the segmentation algorithm incorrectly selects areas that do not belong to the coronary tree. In [3], a particle-based approach to vessel segmentation is performed with interesting results, but non principal branches are missed. Regarding other segmentations methods, we find that level-sets are not suited for real-time applications as they are computationally time-consuming; parametric cylindrical models may not be suited for the non-linear vessel structures and region-growing techniques may be sensitive to local conditions. Because of these difficulties for the accurate detection of the whole coronary tree, we propose to decompose the segmentation task in two different phases; a first phase would deal with the extraction of the coronary tree and in a second phase the coronary substructures would be segmented and classified into regions such as lumen, plaque or calcium. In this paper we propose a solution to the first phase of this scheme using a fast segmentation technique based on mathematical morphology that extracts the 3D coronary tree from an initial seed point given by the human expert. In order not to bias the posterior quantitative segmentation two important requirements for the extraction method should be taken into account: not losing any coronary information and maintaining the local intensity differences. On the other hand we also make the hypothesis that the vessel is a causal structure in the sense that there is no possibility for the artery to grow backwards. It should be noted that the extraction of the coronary tree is very useful on its own as it clearly facilitates the visual inspection of the coronaries with minimal user interaction through longitudinal and transversal sections or using rendering techniques.

This article is organized as follows: firstly, we present the MACTSE (Morphological algorithm for causal tubular structures extraction) algorithm used for the coronary tree extraction giving the implementation details. Then we present and discuss the results on 9 clinical data sets in which the correct extraction of the left coronary arteries has been evaluated by an expert.

2 Morphological Algorithm for Causal Tubular Structures Extraction (MACTSE)

2.1 Theoretical Framework

Mathematical morphology is a nonlinear image processing technique based on geometric analysis that allows to incorporate to the algorithms a priori knowledge of shapes, such as the narrow tubular branching structures of the coronary tree. A tutorial on the technique can be found in [4]. These techniques have been widely used in vessel extraction with successful results [5] and also in segmentation and quantification of 2D angiograms [6,7]. Morphological grayscale reconstruction methods through 2D slice images have been previously used in [8] for the segmentation of the airway tree with successful results. In the case

of the coronary artery tree, the image conditions are different as there are not as many scale changes in the coronary arteries as in bronchia and the existence of other surrounding structures may compromise the segmentation process. In order to solve this challenging problem we propose to use a 2D morphological reconstruction by dilation that is propagated through the slices. A priori information of the coronary radius and the z-axis sampling is used to define the size of the object that is being searched and the area of search in the next slice respectively.

2.2 General Architecture

The proposed procedure can be sketched in the following steps (see fig. 1):

1. The human expert selects a seed point in the first slice where the coronary artery is found.
2. The proposed segmentation method (detailed in section 2.3) is performed from the seed point in the 2D slice i .
3. A set of potential seed points is automatically generated for the morphological segmentation of the slice $i + 1$.
4. Steps 2 and 3 are repeated until there are no potential seeds for the prolongation of the tubular structure.

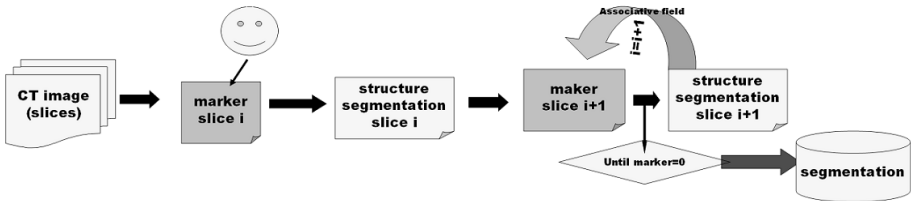


Fig. 1. Scheme of the architecture of MACTSE

2.3 Implementation Details

In order to clarify nomenclature, we introduce some basic morphological operators that can be applied to an image G . The two elementary operations are dilation $\delta_B(G)$ and erosion $\varepsilon_B(G)$ and can be composed together to yield a new set of operators given by opening $\gamma_B(G) = \delta_B[\varepsilon_B(G)]$ and closing $\varphi_B(G) = \varepsilon_B[\delta_B(G)]$. Morphological *openings* (*closings*) filter out light (dark) structures from the images according to the predefined size and shape criterion of the structuring element.

The main morphologic al operator we use is the morphological reconstruction by dilation [9] which consists in an iterative process of geodesic dilations of

the marker image inside the source image until stability. We denote by M the marker image generated from the seed points. The geodesic dilation of size k with structuring element B of the marker image M with respect to the image G is $\delta_G^k(M) = \delta_G^1 \delta_G^{k-1}(M)$, where $\delta_G^1(M) = \delta_B(M) \wedge G$; $\delta_G^1(M)$ indicates a dilation of image M by the structuring element B restricted to G . The reconstruction by dilation of image G from marker M , is denoted $R_B(M, G) = \delta_G^k(M)$ where k is chosen such that $\delta_G^k(M) = \delta_G^{k+1}(M)$ (idempotence).

Hereafter we present the MACTSE algorithm (see an example in fig. 2). Let S_i be the first slice where it is possible to find a coronary artery, M_i the seed selected by the human expert and B_r is a disc structuring element of radius r . MACTSE works as follows:

- A) **Segmentation of the 2D slice S_i .** A reconstruction by dilation is performed on the original image highlighting the marked regions (M_i) (see fig. 3). Then the top-hat opening by reconstruction is used to extract only the bright sections of tubular-like structures (SG_i).
 1. $(IR_i) = R_{B_1}(M_i, S_i)$
 2. $(SG_i) = (IR_i) - R_{B_1}(\gamma_{B_{\mu_1}}(IR_i), IR_i)$
- B) **Generation of potential seed points for the segmentation of slice S_{i+1} .** The new seed points for the following slice segmentation will be generated searching in an area of higher probability that is obtained from the segmentation of slice S_i . We denote this region as associative field A_i and it is created by the dilation of the binary mask of the segmentation of the slice

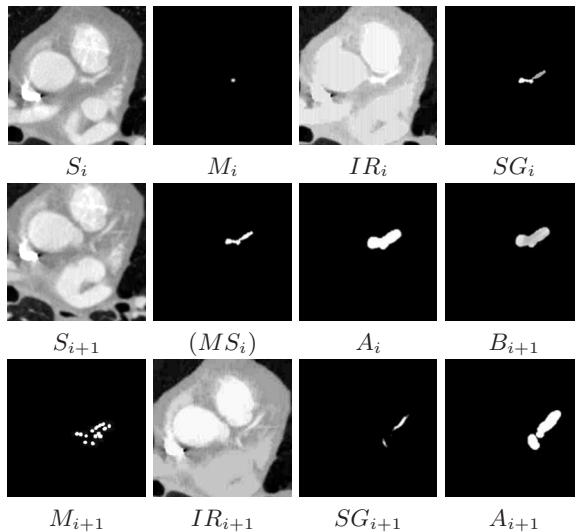


Fig. 2. MACTSE procedure example

S_i thresholding with a value λ . Then the selected seed points correspond to the regional maxima from the intersection of the associative field A_i and S_{i+1} .

3. $(MS_i) = Threshold_\lambda(SG_i)$
4. $(A_i) = \delta_{B_{\mu_2}}(MS_i)$
5. $(B_{i+1}) = (S_{i+1}) \wedge (A_i)$
6. $(M_{i+1}) = RegionalMaxima(B_{i+1})$

C) **Stopping criterion.** The process (A) and (B) are repeated until no potential seed points for the next slices are generated.

7. If $(M_{i+1}) = 0$ then [end] else repeat steps 1 to 6 for $[(M_{i+1}, S_{i+1})]$

Notice that the output is not a binary segmentation, but a grey-level reconstruction of the regions with levels of intensity in each slice corresponding to the difference from the vessel to the background (the plateau around the vessel).

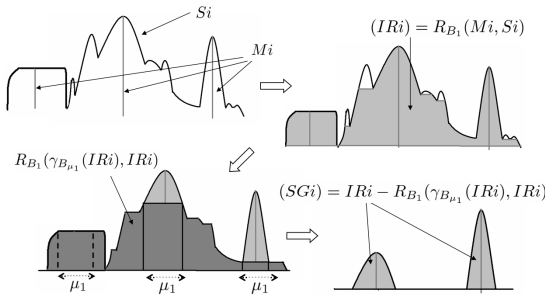


Fig. 3. Scheme of the segmentation of the vessel candidates in one slice

Prior knowledge from the image characteristics is used to adjust the algorithm parameters μ_1 and μ_2 (see fig. 4). These values correspond to the radius of the structuring elements used in the steps 2 and 4. On the one hand, we define the concept of associative field as the region where there is high probability to find the continuation of the vessel. It is adjusted depending on the distance between two slices, $\mu_2 = f(\Delta Z_{slice(i), slice(i+1)})$. This parameter allows tracking the tubular structure even in undersampled z-axis images where the continuation of the tube is not so closely aligned in two consecutive slices. On the other hand, the fact that all the cross-sections of a cylinder have at least one direction of a size equal to the diameter is used to adjust the size parameter μ_1 .

Generally, the segmentation results may be mathematically described as a function of the parameters regarding the property of ordering preservation of morphological operators. These order relationships allow us to construct a hierarchy of embedded segmentations with increasing segmented volume and details by modifying $\mu_1 \uparrow$, $\mu_2 \uparrow$ or $\lambda \downarrow$. Regarding the dependence on the parameters we find that if $\mu_1 \uparrow$ or $\lambda \downarrow$, smaller structures are detected: overdetections may occur and all the small branches are tracked. If $\mu_2 \uparrow$, more potential vessel candidates

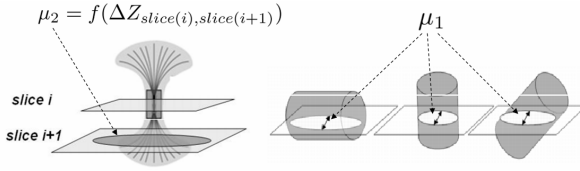


Fig. 4. μ_2 and μ_1 are the radius of the ball structuring elements used to define respectively the associative field and the tubular vessel size

are marked and consequently more details are captured. Modifying parameters in this way allows the user to tune the algorithm easily because of these order relationships and the small variability of each parameter.

3 Coronary Artery Segmentation from CT-Images

3.1 Data Analyzed

The reconstruction algorithm has been tested on 9 3D-MSCT data sets. The images were acquired with a Toshiba Aquilion 16 CT scanner with a slice resolution of $0.5mm$ and a slice spacing of $0.5mm$ (isotropic). Five of the cases present minimal or inexistent lesions. The other four cases present medium or severe problems. The original data has a size of 512×512 in the horizontal plane and between 200 and 300 slices for the z-axis. No pre-processing has been done in the images. The number and length of visible coronary artery segments differs largely in the set of patient data particularly in the pathological cases. We restricted the analysis to the left coronary arteries: the left anterior descending (LAD) coronary artery and the left circumflex (LCX) coronary artery and their branches. The coronary extraction results have been visually evaluated by an expert.

3.2 Extraction Results and Discussion

Table 1 shows the expert evaluation of the severity of the lesions and image quality of the 9 data sets analyzed, together with the assessment of the extraction results. The main branches LAD and LCX are correctly extracted in all cases but patient f . The extraction is satisfactory both for the coronaries without lesions (see fig. 5) and for pathological cases (see fig. 6). The misdetection of LAD in patient f is due to the low image quality, severe lesions and mainly to the presence of a stent that make the signal to be very fuzzy in one slice.

The algorithm parameters have been manually tuned in each case in order to achieve the best reconstruction. In all the cases the optimal choice for the three parameters corresponds to the following range: $\mu_1 \in \{8, 9, 10\}$, $\mu_2 \in \{2, 3, 4\}$, $\lambda \in \{1, 2, 3\}$. A choice of $\mu_1 = 8, \mu_2 = 3, \lambda = 3$ provides acceptable results detecting the main branches in 5 of the cases. The small range of variability of the

Table 1. Segmentation results. Legend: (i) Severity of the pathology: no calcium(1)-multiple lesions(4); (ii) Image quality: bad(1)-excellent(4); (iii) Main branches detection: Yes/No; (iv) Artifacts: No/Ventricular wall - W (in parenthesis the starting point of the artifacts expressed as a proportion of the heart length)/Vein ; (v) Small branches tracking: poor(1)-excellent(4)

Patient	Severity	Image quality	Main branches	Artifacts	Small branches
a	1	3	Yes	V	4
b	1	1	Yes	W($\frac{3}{4}$)	1
c	1	4	Yes	V	3
d	2	4	Yes	No	2
e	2	4	Yes	W($\frac{2}{3}$)	3
f	3,stent	2	NO LAD	No	1
g	4	3	Yes	No	3
h	4	3	Yes	W($\frac{1}{5}$)	3
i	4,stent	3	Yes	W($\frac{3}{4}$)	3

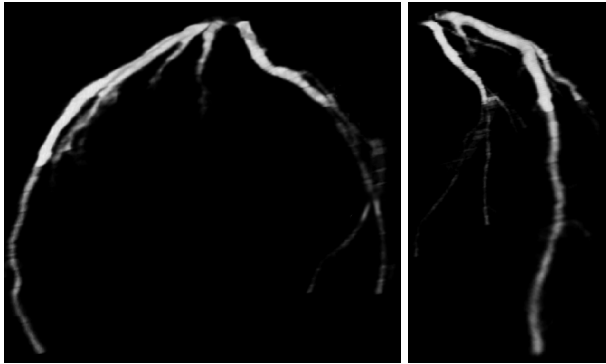


Fig. 5. Left coronary tree without lesions. Video renderings are available at www.die.upm.es/im/videos/CT/.

parameters could be interesting for the implementation of a user interaction interface in order to perform the fine tuning. The main drawback of the algorithm is the extraction in most of the cases of regions that do not correspond to the coronaries in the lowest half of the vessel tree. In cases *b*, *e*, *h*, *i*, these regions correspond to structures located in the low ventricular wall with granulated texture that is interpreted by the algorithm as potential bifurcations of the artery. In cases *a*, *c* a vein that crosses very near the arteries is selected. This overdetection could be avoided tuning the parameters, however the smaller branches wouldn't be detected.

The main advantages of the proposed approach in comparison to other methods, specially those who work with the 3D volume, is its independence from intensity variations during the acquisition procedure. Because of the local nature

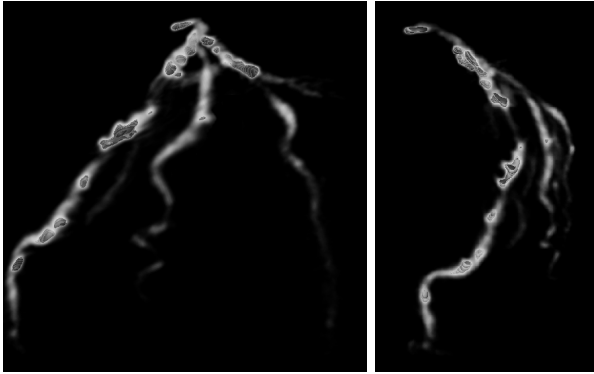


Fig. 6. Left coronary tree with severe calcifications. The isosurfaces superimposed to the rendering are at calcium-level intensity.

of the residues of the morphological reconstruction during the 2D slice analysis, the algorithm is able to follow the arteries in the presence of intensity changes between two slices (which is an important problem for the commercial stations). The algorithm also behaves in a robust way in presence of horizontal shifts between two slices because the associative field permits to track the vessel even if it is misaligned. Concerning computational efficiency, reconstructions are performed in less than 15 seconds in a PentiumIV 3.2GHz, RAM-2GB.

4 Conclusions and Perspectives

The proposed algorithm performs an efficient extraction of the coronary tree from a seed-point initialization. The algorithm is designed to minimize the loss of interesting structures, but in some cases overdetects adjacent regions in the more distal areas of the tree. It behaves in a robust way in the presence of intensity variations or displacement shifts. It works well also in z subsampled volumes, a feature that could be used either to gain speed or to reduce the radiation dose to the patient. A larger validation process including different pathologies should be done. Concerning MACTSE, the most interesting improvement would be to modify the dilation that provides the associative field by deforming the structuring element according to the direction of the vessel in previous frames. Further developments will be devoted to assist in the diagnosis of unhealthy arteries with quantitative data. Current state-of-the-art measurements in order to obtain a quantitative estimation of stenosis or aneurysms are based on cross-sectional areas of vessels at different locations[10]. These measurements are strongly dependent on the estimation of the central axis which is a sensitive task specially in the presence of stenosis. As an alternative methodology, our future workplan is to develop directly a three dimensional classification in the extracted coronary tree based on the Hounsfield density values associated to each tissue and to measure volumetric parameters.

Acknowledgements

This work was supported by the grant FPI-CAM(0362/2005); projects PI041495 and PI041920, from the Spanish Health Ministry; and the CDTEAM project from the CENIT program (Spanish Ministry of Industry).

References

1. Kirbas, C., Quek, F.: A review of vessel extraction techniques and algorithms. *ACM Comput. Surv.* 36, 81–121 (2004)
2. Mueller, D., Maeder, A., O’Shea, P.: Improved direct volume visualization of the coronary arteries using fused segmented regions. In: *DICTA05*, pp. 110–118 (2005)
3. Florin, C., Paragios, N., Williams, J.: Particle filters, a quasi-monte carlo solution for segmentation of coronaries. In: Duncan, J.S., Gerig, G. (eds.) *MICCAI 2005*. LNCS, vol. 3749, pp. 246–253. Springer, Heidelberg (2005)
4. Serra, J.: *Image analysis and mathematical morphology*. Academic Press, London I,II (1982)(1988)
5. Zana, F., Klein, J.: Robust segmentation of vessels from retinal angiography. In: *Int. Conf. on Digital Signal Proc.* pp. 1087–1090. IEEE, New York (1997)
6. Angulo, J., Nguyen-Khoa, T., Massy, F., Drüeke, T., Serra, J.: Morphological quantification of aortic calcification from low magnification images. *Image Analysis and Stereology* 22, 81–89 (2003)
7. Qian, Y., Eiho, S.: Morphological method for automatic extraction of the coronary arteries. *Med. Imaging* 18, 231–238 (2000)
8. Kiraly, A.P., Higgins, W.E., McLennan, G., Hoffman, E.A., Reinhardt, J.M.: Three-dimensional human airway segmentation methods for clinical virtual bronchoscopy. *Academic Radiology* 9, 1153–1168 (2002)
9. Vincent, L.: Morphological grayscale reconstruction in image analysis: efficient algorithms and applications. *IEEE Trans. Image Proc.* 2, 176–201 (1993)
10. Ferencik, M., Lissauskas, J.B., Cury, R.C., Hoffmann, U., Abbara, S., Karl, W.A.S., Brady, T.J., Chan, R.C.: Improved vessel morphology measurements in mdct coronary angiography with non-linear post-processing. *Eur. J. Radiology* 57, 380–383 (2006)